Optics Communications 330 (2014) 40–44

Contents lists available at ScienceDirect

Optics Communications

journal homepage: www.elsevier.com/locate/optcom

Hybrid amorphous silicon (a-Si:H)–$LiNbO_3$ electro-optic modulator

Liang Cao [a,*], Abdelsalam Aboketaf [a], Zihao Wang [a], Stefan Preble [a,b]

[a] Rochester Institute of Technology, Microsystems Engineering, Kate Gleason College of Engineering, Rochester Institute of Technology, Rochester, NY 14623, USA

[b] Rochester Institute of Technology, Electrical & Microelectronic Engineering, Kate Gleason College of Engineering, Rochester Institute of Technology, Rochester, NY 14623, USA

ARTICLE INFO

Article history:
Received 27 February 2014
Received in revised form
6 May 2014
Accepted 6 May 2014
Available online 22 May 2014

Keywords:
$LiNbO_3$
Modulator
Silicon photonics
Hybrid

ABSTRACT

Here we report the demonstration of a GHz-speed Lithium Niobate ($LiNbO_3$) modulator that uses an amorphous Silicon waveguide to strongly confine light. The compact (<1 mm) modulator is realized by low-temperature deposition of hydrogenated amorphous Silicon (a-Si:H) onto a x-cut $LiNbO_3$ substrate. The a-Si:H provides tight waveguide mode confinement while allowing strong evanescent coupling to the underlying $LiNbO_3$ substrate which, in turn, enables efficient electro-optic modulation. This approach overcomes the traditional drawbacks of low-index contrast $LiNbO_3$ waveguides and consequently is able to realize a strong Pockels effect in a densely integrated Silicon photonics platform. It is expected that this new Si–$LiNbO_3$ platform will enable a multitude of devices and circuits for RF Photonics, nonlinear optics and quantum optics.

1. Introduction

The Silicon photonics platform has shown great promise for next generation photonic integrated circuits. Its success is primarily attributed to high performance electro-optic modulators based on the free-carrier plasma dispersion effect. However, Lithium Niobate modulators, based on the Pockels effect, offer several advantages, including, a purely linear electro-optic response, no free carrier absorption loss, a simpler fabrication process (no need for multiple ion implantations and anneals), and the highest bandwidths to date (>300 GHz [1]). As a result there have been many efforts to realize strong $\chi(2)$ nonlinear optical effects in the high index contrast Silicon photonics platform. For example, a significant Pockels effect was realized in Silicon by using strain to break the crystal symmetry [2,3]. In other cases, $\chi(2)$ materials, such as nonlinear polymers [4,5] or Aluminum Nitride [6] have been deposited and used to enable electro-optic modulation. In contrast, the major drawback of Lithium Niobate ($LiNbO_3$) platform is the low index contrast of standard Titanium diffused Lithium Niobate waveguides (Ti:$LiNbO_3$). Consequently, it is challenging to realize densely integrated photonic circuits on the $LiNbO_3$ platform. Some work has been done to either etch $LiNbO_3$ [7,8] or deposit high index chalcogenide glasses [9]. However, the devices are still an order of magnitude larger than their Silicon photonic counterparts. In order to overcome this some groups have recently bonded $LiNbO_3$ films onto Silicon waveguides or substrates [10–14]. However, these approaches require additional ion implantation and bonding steps [15]. In contrast, here we combine the high index contrast of Silicon photonics and $LiNbO_3$ by simply depositing high index hydrogenated amorphous Silicon (a-Si:H) on $LiNbO_3$ substrates in order to realize a compact and efficient active hybrid Silicon:$LiNbO_3$ platform. This platform will enable a multitude of ultra-high performance photonic integrated circuits for communications and RF signal processing. In addition, the $\chi(2)$ nonlinearity can be leveraged for quantum and nonlinear optics applications.

Our group has previously shown that the loss of plasma enhanced chemical vapor deposited (PECVD) hydrogenated amorphous Silicon (a-Si:H) waveguides can be similar to crystalline Silicon [16]. Specifically, recent demonstrations have shown <3 dB/cm loss on thermal oxide [17] or ITO glass substrates [18]. Furthermore, the amorphous silicon waveguides have nearly the same refractive index as crystalline Silicon waveguides ($\sim$3.45) and there has been thorough research of transmission loss for different processing temperature [17], therefore, it is possible to realize very compact photonic circuits by simply depositing a-Si:H at temperatures lower than 400 °C. And hydrogenated amorphous Silicon has been used to enhance the waveguide refractive index of $BaTiO_3$ devices [19]. Here we present our results on a hybrid a-Si:H–$LiNbO_3$ modulator where the same a-Si:H material is deposited on a $LiNbO_3$ substrate. We have optimized the a-Si:H waveguide dimensions in order to maximize the

* Corresponding author.
E-mail address: sfpeen@rit.edu (S. Preble).

http://dx.doi.org/10.1016/j.optcom.2014.05.021
0030-4018/

overlap of the optical mode with the electro-optically active $LiNbO_3$ material. As a result, it is possible for ~75% of the mode to sense an electrically induced refractive index change in the $LiNbO_3$ material. Furthermore, since the optical mode is strongly confined to the a-Si:H waveguide width (<1 μm), the electrodes can be placed very closely together, significantly enhancing the applied electric field. As a result, it is possible to realize an electro-optic modulator with less than 2 V-cm response, nearly an order of magnitude smaller than typical. Here we show a proof of concept and demonstrate >4 GHz modulation in a small footprint of <1 mm.

2. Device design and simulation

A schematic of the proposed hybrid a-Si:H/$LiNbO_3$ waveguide modulator is shown in Fig. 1, where an a-Si:H waveguide core is patterned on top of a $LiNbO_3$ substrate. The TE optical mode for this a-Si:H waveguide (700 nm wide, 90 nm thick) is superimposed in the image along with the simulated electric field induced by applying a voltage to the metal electrodes. The strong lateral optical confinement of the a-Si:H waveguide ensures that the metal electrodes can be spaced closely together (3 μ in this figure). Furthermore, the thin a-Si:H material allows a significant amount of the optical mode to strongly sense the $LiNbO_3$ substrate. Therefore, it is possible to obtain both low voltage and compact electro-optic modulation in this hybrid platform.

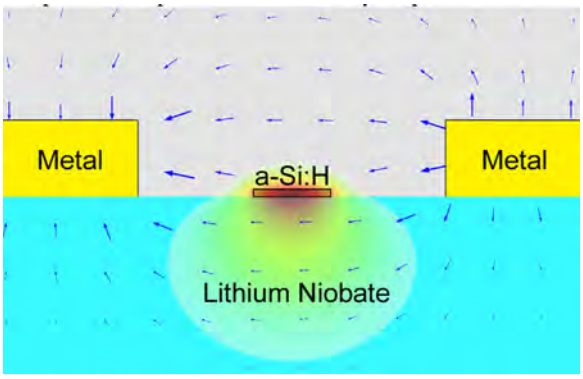

Fig. 1. Schematic cross-section of the hybrid Silicon–$LiNbO_3$ modulator. The light is confined to the $LiNbO_3$ substrate by a thin a-Si:H waveguide in TE mode. The metal electrodes provide an RF electric field that is used to induce the Pockels effect in the $LiNbO_3$.

In order to enhance the overall Pockels modulation effect we need to ensure as much of the optical mode is in the $LiNbO_3$ region as possible. At the same time, we need to make sure that the optical mode is compact, so that devices can be realized with significantly smaller footprints. This can be well understood from the TE mode simulations shown in Fig. 2(a–d). In all cases the waveguide has a 700 nm width but it is clearly seen that in order to realize an appreciable amount of light in the $LiNbO_3$ substrate the a-Si:H must be relatively thin, approximately less than 100 nm.

To further investigate the influence of the profile of optical mode on the modulation strength, a series of simulations are summarized in Fig. 3(a). We have once again fixed the width of the waveguide to be 700 nm and varied the a-Si:H thickness from 80 nm to 200 nm. At each thickness, we calculate the efficiency of the effective refractive index change in the $LiNbO_3$ material, which is simply obtained by applying a small change to the $LiNbO_3$ refractive index and seeing the net change in the overall effective index of the mode. As we can see from the blue curve in Fig. 3 (a) the effective index change from the $LiNbO_3$ modulation increases as the waveguide becomes thinner. This is simply because the amount of light in the $LiNbO_3$ increases as the waveguide is thinned. However, there is a limit to how thin it can be made, which in this specific waveguide width is approximately a thickness of 80 nm. It is at this point that the effective index (red curve in Fig. 3(a)) reaches the same value as the $LiNbO_3$ substrate, and consequently the mode is no longer strongly confined by the a-Si:H waveguide and will be very leaky. Fig. 3 (b) looks at the dependence on the waveguide width for several a-Si:H thicknesses. As we can see, all of the curves follow the same general trend, specifically that thinner waveguides enhance the modulation effect. However, as the waveguides get narrower the

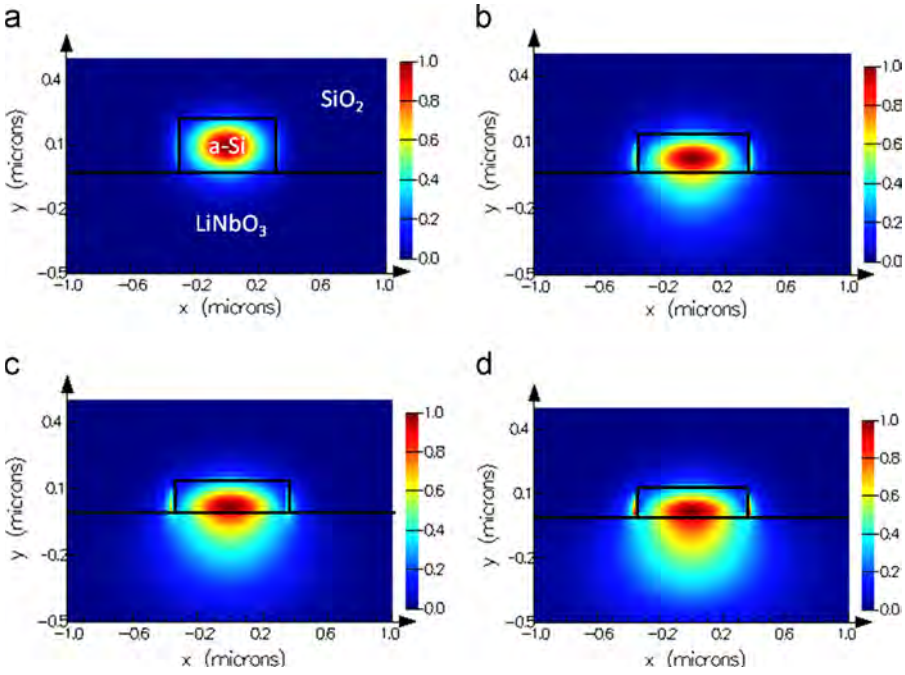

Fig. 2. Optical mode (TE) of a-Si:H waveguide on a $LiNbO_3$ substrate (a) waveguide thickness 200 nm, (b) waveguide thickness 100 nm, (c) waveguide thickness 80 nm, (d) waveguide thickness 70 nm.

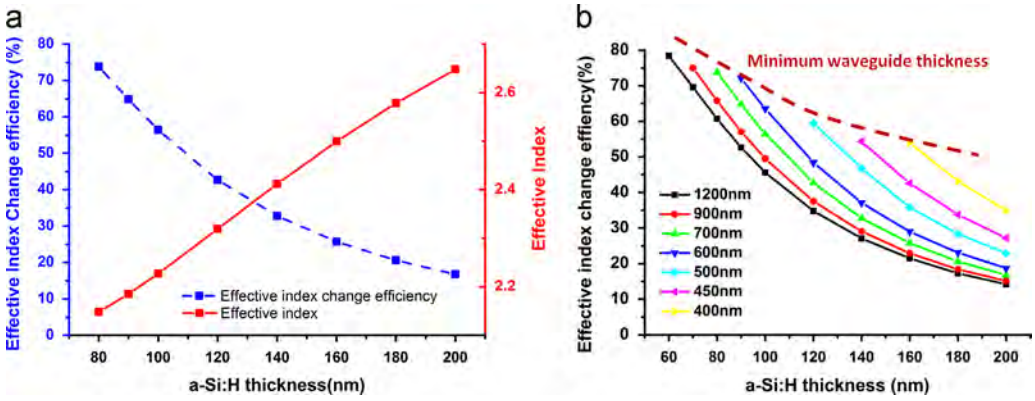

Fig. 3. (a) Relative index change efficiency for a 700 nm wide waveguide for different a-Si:H thicknesses. (b) Waveguide width dependence on index change efficiency.

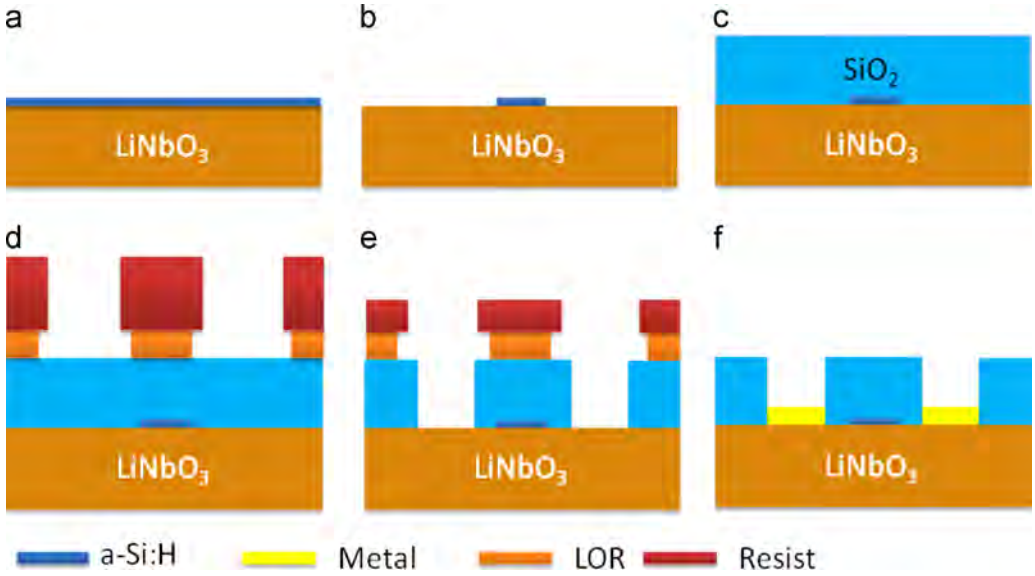

Fig. 4. Fabrication process of hybrid Si–$LiNbO_3$ electro-optic modulator.

required waveguide thickness increases and as a result the ultimate effective index change efficiency that can be obtained is decreased. Therefore, it is better to have wider waveguides to reach the ultimate modulation efficiency. However, there is a tradeoff in minimum bend radius as the waveguide is made wider and thinner, as comprehensively explored in [20]. As a result, we have selected the 700 nm width as a reasonable tradeoff point since it provides good modulation efficiency and low loss bends with a radius as small as ~15 μ for the TE polarization of light [20].

Table 1
a-Si:H deposition parameter.

Hydrogen (H2) flow	700 sccm
Silane (SiH4) flow	60 sccm
RF Power	100 W
Substrate temperature	200 °C
Pressure	4 Torr

3. Fabrication

Here we present the process for fabrication of a proof-of-principle hybrid Silicon–$LiNbO_3$ modulator. The fabrication starts from an x-cut $LiNbO_3$ wafer, which will yield the maximum Pockels coefficient (r_{33}) for the lateral metal electrode configuration presented in Fig. 1. Then a-Si:H is deposited using plasma enhanced chemical vapor deposition (PECVD) at 200 C, as depicted in Fig. 4(a). The deposition parameters of the film are given in Table 1 [16]. Then the strip waveguides, 700 nm wide, are patterned using electron beam lithography followed by inductively coupled plasma (ICP) chlorine etch similar to our standard silicon waveguide fabrication process [21]. After the a-Si:H is fully etched, 1 μm of SiO_2 is deposited over the structure also using PECVD at a temperature of 400 °C as shown in Fig. 4(c). Next, contact holes are patterned using contact lithography as shown in Fig. 4(d) and followed by RIE etching of SiO_2. Then the contact hole is filled with 100 nm of gold. Finally, lift-off of the electrode metal is performed in an acetone bath (Fig. 4f). Lastly, we note that it is possible to realize these devices with even lower temperature deposition processes, since it has been shown that it is possible to deposit a-Si:H at room temperature [22].

In order to convert the electric field induced refractive index change into an optical intensity change, the waveguides are patterned into a Mach–Zehnder Interferometer (MZI) configuration as shown in Fig. 5. The modulation region of the device is ~800 μm long which is much smaller than traditional $LiNbO_3$ MZI modulators. Furthermore, there is ~100 μm length difference in one branch of the MZI in order to directly obtain the modulation induced phase change from the wavelength-dependent transmission of the MZI, as shown in the results section.

4. Results and discussion

The experimental setup used to measure the modulation efficiency is shown in Fig. 6. Optical measurements are performed using a tunable infrared laser that passes through a polarization controller, a collimator and a lens focused on the chip facet. Light is efficiently coupled in and out of the chip via nanotaper mode converters [23]. The output from the chip is collimated by the lens and is collected by another collimator. The light is detected by a photodetector in order to obtain the transmission spectrum of the MZI by scanning the tunable lasers wavelength. Alternatively the output signal is amplified by an Erbium Doped Fiber Amplifier (EDFA) and measured by an optical detection module in a sampling oscilloscope. The modulator is electrically biased by DC probes and an RF probe that is driven by a tunable RF source.

The optical loss of the waveguides was observed to be similar to previously fabricated a-Si:H waveguides on SiO_2 ($\sim$3 dB/cm [16]) by visualizing light scattering using an infrared camera. However, an exact waveguide loss was not possible to determine because the current waveguides are too short ($\sim$2 mm). Furthermore, the imaginary refractive index (k) of the deposited a-Si:H was not possible to directly obtain using ellipsometry because the deposited film was too thin and exhibited relatively low loss (expected to be $<$3 dB/cm). In the future it will be advantageous to optimize the fabrication process in order to obtain very low loss waveguides ($<$3 dB/cm), as has been done on other substrates [17,18].

DC analysis is performed by measuring the devices spectral response for various applied electric fields. The DC bias is operated in a push and pull configuration, where the DC voltage is applied to the center electrode and the two outside electrodes are grounded. Since the Pockels effect induces either a positive or negative index change based on the direction of the electric field, the effective phase change of the MZI is doubled in this configuration. The spectral response at various electric fields is shown in Fig. 7, where the blue line is the spectrum without bias. It is seen that the MZI has a high extinction of 20 dB and the 100 μ length

Fig. 5. Microscope image of the hybrid Si–$LiNbO_3$ modulator integrated into a Mach–Zehnder interferometer. The total size of the device is only 1 mm.

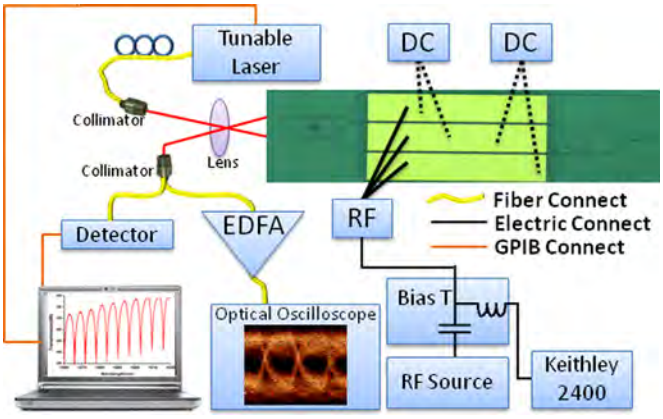

Fig. 6. Experimental setup used to characterize the MZI modulator.

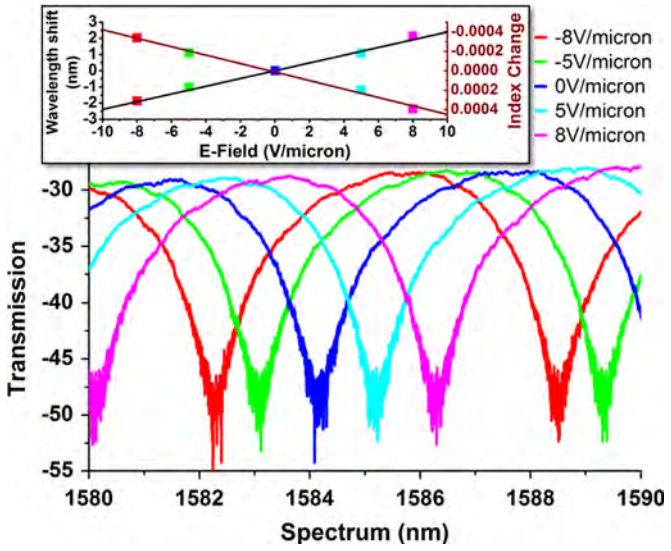

Fig. 7. Spectral change induced by DC electric field. The upper inset shows the wavelength change and the corresponding effective index change.

difference yields a Free-Spectral-Range of 6.2 nm. It is also seen that there is a linear shift in the wavelength spectra for different Electric fields as expected from the $LiNbO_3$ Pockels effect. However, the overall switching field (defined as the field required to obtain a π phase shift) of the modulator is relatively high, approximately 10 V/μ. Since contact lithography was used to pattern the electrodes, they are separated much farther than necessary (11 μ), which results in a relatively high measured $V_{\pi L}\sim$8.8 V-cm. In addition, we determined that the effective Pockels coefficient of our waveguide configuration is only $\sim$10 pm/V, whereas bulk $LiNbO_3$ material has an r_{33}=33 pm/V. The primary reason we do not reach the optimal efficiency is because the deposited a-Si:H was found to be 150 nm thick, significantly thicker than anticipated. As seen in Fig. 3(a), only $\sim$30% of the optical mode is sensing the $LiNbO_3$ refractive index change, which confirms the measured 10 pm/V efficiency. In the future, by reducing the waveguide thickness to $<$100 nm it will be possible to realize an increase in modulation efficiency. In turn, the overall performance of this new type of hybrid modulator can be calculated using the standard $V_{\pi L}$ figure of merit. Specifically, assuming the electrodes can be conservatively spaced 3 μ apart, which induces negligible optical loss, and that the r_{33} is even only modestly increased ($1.5x$–$r_{33}\sim$15 pm/V) then the switching voltage can be approximately $V_{\pi L}\sim$1.6 V-cm, which is significantly smaller than typical $LiNbO_3$ modulators [24]. Therefore, with this new hybrid waveguide approach it is possible to realize significantly smaller modulators with a simple Silicon deposition waveguide process.

We have also measured the RF response of the modulator as seen in Fig. 8 by sweeping an RF source from 100 MHz to 13 GHz. The modulated optical signal is measured as a function of frequency using a sampling oscilloscope with a 30 GHz bandwidth photoreceiver module. The resulting data is given in Fig. 8, which shows that the MZI modulator has a 3-dB roll-off frequency of $\sim$2.5 GHz. We note that the cause of the $\sim$1 dB oscillations is currently unclear and believe it may be due to the unoptimized RF electrode design (impedance mismatch and multimode behavior) along with the modulation (accumulation/depletion) of free-carriers in the a-Si:H material. These factors may also be limiting the RF speed and we are continuing the analyze the ultimate bandwidth of the device. Regardless, we are still able to achieve an open eye diagram at 4.5 Gb/s by applying a Non-Return-to-Zero

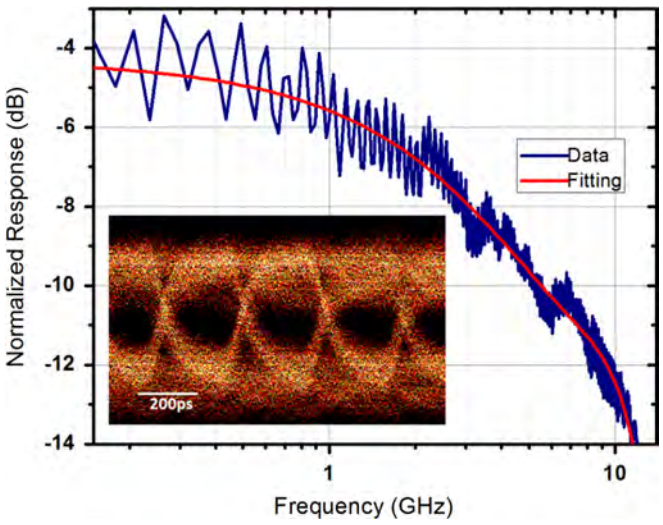

Fig. 8. RF response of the modulator for different frequencies. The inset shows an open eye-diagram for a 4.5 Gb/s PRBS 2^7-1 signal.

(NRZ) 2\widehat7-1 Pseudo Random Bit Sequence using an RF signal with a ± 5 V swing as shown in the bottom left inset of Fig. 8.

5. Conclusions

We have demonstrated a hybrid Silicon–$LiNbO_3$ modulator that utilizes a simple amorphous Silicon deposition process to realize both tight confinement of the optical mode and strong modulation efficiency. Consequently, this work has shown that it may be possible to realize significantly smaller $LiNbO_3$ modulators that operate with low voltages (<2 V-cm). Additional modeling work is required to determine the ultimate bandwidth of the modulators but it is expected that that since the device utilizes the instantaneous Pockels effect in $LiNbO_3$ it will be possible to realize ultra-fast modulators that are highly linear and have low loss. Furthermore, the integration approach can be used to realize a multitude of other compact and low loss devices that are seamlessly integrated on a single platform.

Acknowledgements

We would like to thank Dr. Gernot Pomrenke of the Air Force Office of Scientific Research for his support under FA9550-10-1–0217. This work was also partially supported by NSF under Award # 1315369. This work was performed in part at the Cornell NanoScale Facility, a member of the National Nanotechnology Infrastructure Network, which is supported by the National Science Foundation (Grant no. ECS-0335765).

References

[1] J. Macario, P. Yao, S. Shi, A. Zablocki, C. Harrity, R.D. Martin, C.A. Schuetz, D.W. Prather, Opt. Express 20 (21) (2012) 23623.
[2] B. Chmielak, M. Waldow, C. Matheisen, C. Ripperda, J. Bolten, T. Wahlbrink, M. Nagel, F. Merget, H. Kurz, Opt. Express 19 (2011) 17212.
[3] R.S. Jacobsen, K.N. Andersen, P.I. Borel, J. Fage-Pedersen, L.H. Frandsen, O. Hansen, M. Kristensen, A.V. Lavrinenko, G. Moulin, H. Ou, C. Peucheret, B. Zsigri, A. Bjarklev, Nature 441 (2006) 199.
[4] D. Korn, R. Palmer, H. Yu, P.C. Schindler, L. Alloatti, M. Baier, R. Schmogrow, W. Bogaerts, S.K. Selvaraja, G. Lepage, M. Pantouvaki, J.M.D. Wouters, P. Verheyen, J. Van Campenhout, B. Chen, R. Baets, P. Absil, R. Dinu, C. Koos, W. Freude, J. Leuthold, Opt. Express 21 (2013) 13219.
[5] L. Alloatti, D. Korn, R. Palmer, D. Hillerkuss, J. Li, A. Barklund, R. Dinu, M. Fournier, J. Fedeli, H. Yu, W. Bogaerts, P. Dumon, R. Baets, Opt. Express 19 (2011) 11841.
[6] C. Xiong, W.H.P. Pernice, H.X. Tang, Nano Lett. 12 (2012) 3562.
[7] H.H.H. Hu, R.R.R. Ricken, W.S.W. Sohler, R.B.W.R.B. Wehrspohn, IEEE Photonics Technol. Lett. 19 (2007).
[8] H. Lu, F. Issam Baida, G. Ulliac, N. Courjal, M. Collet, M.-P. Bernal, Appl. Phys. Lett. 101 (2012) 151117.
[9] M.E. Solmaz, D.B. Adams, W.C. Tan, W.T. Snider, C.K. Madsen, Opt. Lett. 34 (2009) 1735.
[10] P. Poberaj, G. Hu, H. Sohler, W. Günter, Laser Photonics Rev. 6 (4) (2012) 488.
[11] S. Darmawan, L.Y.M. Tobing, T. Mei, Opt. Lett. 35 (2010) 238.
[12] Y.S. Lee, G.-D. Kim, W.-J. Kim, S.-S. Lee, W.-G. Lee, W.H. Steier, Opt. Lett. 36 (2011) 1119.
[13] L. Chen, R.M. Reano, Opt. Express 20 (2012) 4032.
[14] L. Chen, M.G. Wood, R.M. Reano, Opt. Express 21 (2013) 27003.
[15] P. Rabiei, J. Ma, S. Khan, J. Chiles, S. Fathpour, Opt. Express 21 (2013) 114.
[16] K. Narayanan, S.F. Preble, Opt. Express 18 (9) (2010) 8998.
[17] S. Zhu, G.Q. Lo, D.L. Kwong, Opt. Express 18 (2010) 25283.
[18] S. Rao, F.G. Della Corte, C. Summonte, J. Eur. Opt. Soc. 5 (2010).
[19] C. Xiong, W. Pernice, J. Ngai, J. Reiner, D. Kumarh, F. Walker, C. Ahn, H. Tang, Nano Lett. (2014) 1.
[20] S.C.K. Mehmet, Madsen, Proc. SPIE 6386 (63860F) (2006).
[21] L. Cao, A.A. Aboketaf, S.F. Preble, Opt. Commun. 305 (2013) 66.
[22] P. Alpuim, V. Chu, J. Conde, J. Non-Cryst. Solids 266–269 (2000) 110.
[23] V.R. Almeida, R.R. Panepucci, M. Lipson, Opt. Lett. 28 (2003) 1302.
[24] D. Janner, D. Tulli, M. Belmonte, V. Pruneri, J. Opt. A: Pure Appl. Opt. 10 (2008) 104003.